*31st EPS Conference on Plasma Phys. London, 28 June - 2 July 2004 ECA Vol.**28G**, P-4.203 (2004)*

Magnetic Prandtl Number Effects in MHD Turbulence

John V. Shebalin

Advanced Space Propulsion Laboratory, Houston, Texas 77058 USA

The magnetic Prandtl number P_M is defined as the ratio between the kinematic viscosity ν and the magnetic diffusivity η: $P_M \equiv \nu/\eta$. The transport coefficients ν and η appear in the evolution equations for fluid velocity **u** and magnetic field **b** in a turbulent magnetofluid. Here, we will address only two-dimensional (2-D), incompressible, magnetohydrodynamic (MHD) turbulence, where $\nabla\cdot\mathbf{u} = 0 = \nabla\cdot\mathbf{b}$, so that $\mathbf{u} = \nabla\times(\psi\hat{\mathbf{e}}_z)$ and $\mathbf{b} = \nabla\times(a\hat{\mathbf{e}}_z)$. The vorticity of the fluid is $\boldsymbol{\omega} = \omega\hat{\mathbf{e}}_z = \nabla\times\mathbf{u}$ and the current is $\mathbf{j} = j\hat{\mathbf{e}}_z = \nabla\times\mathbf{b}$, where we have the vorticity scalar $\omega = -\nabla^2\psi$ and electric current $j = -\nabla^2 a$. The well-known (dimensionless) equations for ω and the magnetic potential a are

$$\text{(a)}\ \frac{\partial\omega}{\partial t} + \mathbf{u}\cdot\nabla\omega = \mathbf{b}\cdot\nabla j + \nu\nabla^2\omega \qquad \text{(b)}\ \frac{\partial a}{\partial t} + \mathbf{u}\cdot\nabla a = \eta\nabla^2 a \qquad (1)$$

Here, we exclude the possibility of a 2-D mean magnetic field $\mathbf{B}_o$. Equations (1a) and (1b) thus determine the evolution of $\omega(\mathbf{x},t)$ and $a(\mathbf{x},t)$ in terms of position **x** and time t.

We further assume the flow is homogeneous, so that a Fourier representation[1] of the dynamic variables ω and a can be used. Doing so transforms the two partial differential equations in (1) into a very large number of ordinary differential equations ($\sim 4\times10^5$ for a 512^2 grid) for the Fourier modes $\omega(\mathbf{k},t)$ and $a(\mathbf{k},t)$, where **k** is a wave vector with integer components. These o.d.e.s are then numerically integrated by a third-order Adams-Bashforth technique[2]. (For further details and references see[3].)

Equations (1) can be solved for the case of ideal flows ($\nu = \eta = 0$) or for real flows ($\nu > 0$, $\eta > 0$). In the ideal case, a statistical solution in terms of canonical ensembles is known[4], while in the real case, there is no such statistical solution. In both cases a numerical solution is straightforward. In the ideal case there is a discrepancy between canonical ensemble predictions and numerical simulation (*i.e.*, time averages), which is explained through the mechanism of broken ergodicity[5,6]. Briefly, the canonical ensemble theory predicts a zero-mean value for all Fourier modes, while numerical simulations show that this is not so. The explanation[6] lies in the fact that the equations of motion and the statistical theory are invariant under the classical discrete symmetry operations C, P and T (charge conjugation, parity transformation and time reversal, respectively), but time evolution, and hence time

averages, are not invariant (due to the presence of ideal constants of the motion such as cross helicity and magnetic helicity, which are pseudoscalars under *C* and *P*). Thus the symmetry of the theory is dynamically broken, leading to non-ergodicity. Combining these concepts gives us *broken ergodicity*, which manifests itself in the phase space of the ideal dynamical system through the presence of disjoint invariant sets, the number of these sets being 2^M, where M is the number of helical invariants in the ideal MHD turbulence under study. For the ideal 2-D case, $M = 1$, so that there are two disjoint invariant sets in phase space and in the 3-D case with $\mathbf{B}_o = 0$, $M = 2$, hence four disjoint invariant sets[7].

In a real case, there is dissipation and thus there are no constants of the motion on which to base a canonical ensemble theory. In order to determine if broken ergodicity is present in real MHD turbulence, eight separate numerical runs were made with varying values of ν and η. The simulation set consisted of one ideal run and seven real runs. All runs had equivalent initial conditions (*i.e.*, equal and non-zero Fourier modes for $k^2 \leq 58254$). The dimensions of the associated dynamical systems were 366104 in the ideal simulation (spectral, $k^2_{max} = 58254$), and 411712 in the real simulations (pseudospectral, $k^2_{max} = 65535$). Table I gives the values of ν, η, the magnetic Prandtl number $P_M = \nu/\eta$, and t_{final} for each of these eight runs (the ideal case is denoted by $P_M =$ '0/0').

Table I. Parameters for the numerical simulations

Run	ν	η	P_M	t_{final}
I1	0	0	0/0	25
R1	0.001	0.010	0.100	25
R2	0.001	0.004	0.250	25
R3	0.0025	0.0025	1.000	25
R4	0.004	0.001	4.000	25
R5	0.001	0.008	0.125	15
R6	0.001	0.00625	0.160	15
R7	0.001	0.005	0.020	15

The initial conditions were such that the initial kinetic and magnetic energies (E_K and E_M), cross helicity (H_C), and mean square magnetic potential (A) were the same for all runs: $E_K = E_M = 0.5$, $H_C = 0.024613$, $A = 0.031031$ at $t = 0$. The initial values of the complex coefficients $\omega(\mathbf{k})$ and $j(\mathbf{k})$ had random phase and magnitudes that varied as $|\omega(\mathbf{k})| = |j(\mathbf{k})| \sim k^3 \exp(-k^2/16)$. These initial values gave initial energy spectra $E_K(k) = E_M(k) \sim k^6 \exp(-k^2/8)$, *i.e.*, spectra that were highly peaked around $k^2 = 5$. The time step for numerical integration was $\Delta t = 10^{-4}$, and each run in Table I was taken to $t = 25$ or to $t = 15$. Each time step for the

ideal run took about 9 cpu-seconds (because of dealiasing), while the time steps for the real runs took about 5 seconds each.

Essential results are shown in the figures. Figure 1 shows the representative Fourier mode $a(\mathbf{k})$, with $\mathbf{k} = (0,1)$, evolving from $t = 0$ to $t = 25$ for the runs I1 and R1 – R4. Other Fourier modes also have non-zero means, in contrast to ideal ensemble predictions. In fact, at low k, the $a(\mathbf{k})$ grow (by inverse cascade and selective decay[8]) to mean values (through broken ergodicity[5,6,7]) that are large compared to fluctuations about those means. Furthermore, in Figure 2, energy spectra for runs I1 and R1 – R4, at $t = 25$, show that while ideal and real runs vary at high k, they are similar at low k.

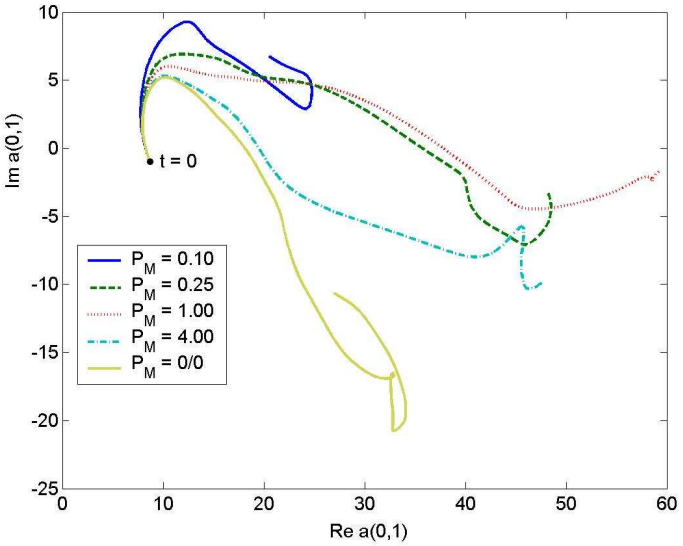

Figure 1. Evolution of $a(\mathbf{k})$, $\mathbf{k} = (0,1)$.

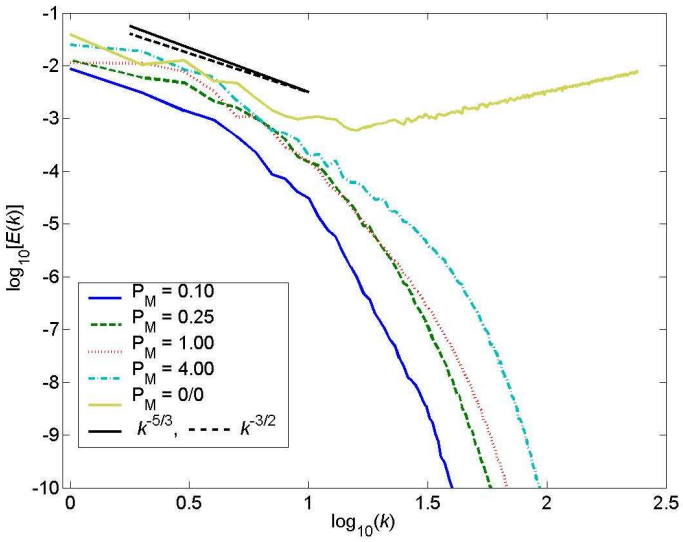

Figure 2. Ideal and real energy spectra at $t = 25$.

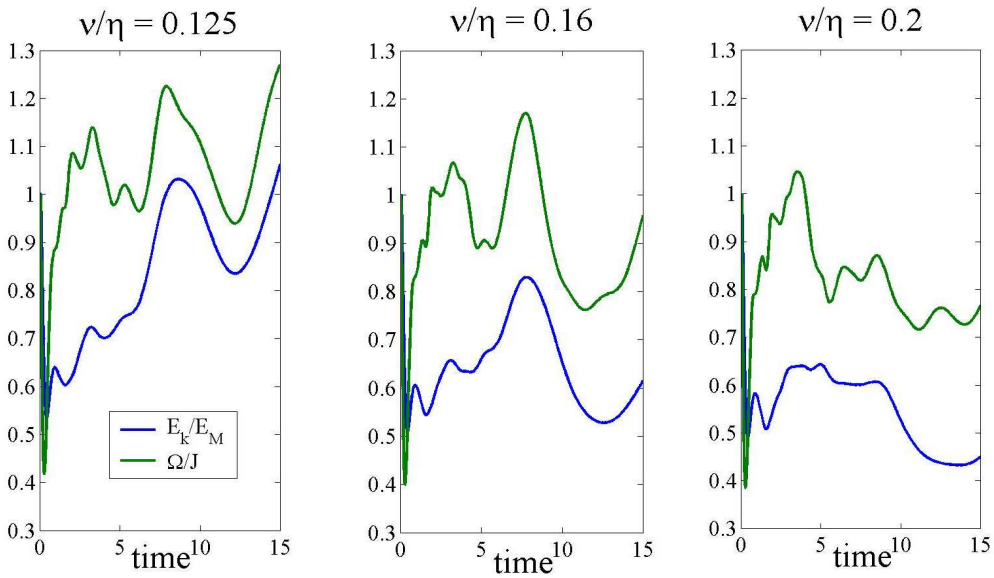

Figure 3. Ratios of kinetic to magnetic quantities for runs R5, R6 and R7.

In Figure 3, the ratios of kinetic energy E_k to magnetic energy E_m, and of enstrophy Ω to mean square current J, show that these are more equal at $P_M \cong 1/8$ than at the customary computationally chosen value of $P_M = 1$. (However, there have been recent simulations at very low P_M done by other researchers[9].) Also, Figure 3 suggests that the ratio of viscous to ohmic dissipation, $\nu\Omega/\eta J = P_m\,\Omega/J$, may be roughly constant.

In summary, the broken ergodicity that was discovered to exist in ideal turbulence is manifest in dissipative turbulence in the range of P_M considered here. In particular, the low-k parts of the turbulent energy spectra (*i.e.*, the large eddies) show strong similarity with ideal simulations. Two major implications are that turbulence theories and models may need to incorporate non-zero mean values, and that large-scale astro- and geomagnetic fields may be due, in essence, to inverse cascade and broken ergodicity.

[1]J. P. Boyd, *Chebyshev and Fourier Spectral Methods*, 2nd Ed., (Dover, Mineola, NY, 2001).

[2] J. Gadzag, Time-differencing schemes and transform methods, *J. Comp. Phys*. **20**, 196 (1976).

[3]J. V. Shebalin, *The statistical mechanics of ideal homogeneous turbulence*, NASA TP-2002-210783, (NASA JSC, Houston, TX, 2002).

[4]D. Fyfe & D. Montgomery, High beta turbulence in two-dimensional magneto-hydrodynamics, *J. Plasma Phys*. **16**, 181–191 (1976).

[5]J. V. Shebalin, Broken ergodicity and coherent structure in homogeneous turbulence, *Physica D*, **37**, 173-191 (1989).

[6]J. V. Shebalin, Broken symmetry in ideal magnetohydrodynamic turbulence, *Phys. Plasmas*, **1**, 541-7 (1994).

[7]J. V. Shebalin, Phase space structure in ideal homogeneous turbulence, *Phys. Lett. A*, **250**, 319-322 (1998).

[8]D. Biskamp, *Magnetohydrodynamic Turbulence*, pp 75-77 (Cambridge U. P., UK, 2003).

[9]Y. Ponty, H. Politano & J.-F. Pinton, Simulation of Induction at Low Magnetic Prandtl Number, *Phys. Rev. Lett.* **92**, 144503-1 (2004).